




Article

A Novel Approach for Enhanced Osteosarcoma Photodynamic Therapy Using Encapsulated Methylene Blue in Silica Nanoparticles

Khaled Al Jarrah ^{1,*}, M-Ali H. Al-Akhras ^{1,*}, Ghaseb N. Makhadmeh ¹, Tariq AlZoubi ^{2,*} , Abdulsalam Abuelsamen ³, Samer H. Zyoud ⁴, Mohammad A. Mhareb ⁵, Azlan Abdul Aziz ⁶ and Osama Abu Noqta ¹

- ¹ Physics Department, Biomedical Physics Laboratory, Jordan University of Science and Technology, Irbid 22110, Jordan
 - ² College of Engineering and Technology, American University of the Middle East, Egaila 54200, Kuwait
 - ³ Medical Imaging and Radiography Department, Aqaba University of Technology, Aqaba 910122, Jordan
 - ⁴ Nonlinear Dynamics Research Center (NDRC), Department of Mathematics and Sciences, Ajman University, Ajman P.O. Box 346, United Arab Emirates
 - ⁵ Department of Physics, College of Science, Imam Abdulrahman Bin Faisal University, Dammam 31441, Saudi Arabia
 - ⁶ Nano-Biotechnology Research and Innovation (NanoBRI), Institute for Research in Molecular Medicine (INFORMM), Universiti Sains Malaysia, Pulau Pinang 11800, Malaysia
- * Correspondence: kjarrah@just.edu.jo (K.A.J.); alakmoh@just.edu.jo (M.-A.H.A.-A.); tariq.alzoubi@aum.edu.kw (T.A.)



Citation: Al Jarrah, K.; Al-Akhras, M.-A.H.; Makhadmeh, G.N.; AlZoubi, T.; Abuelsamen, A.; Zyoud, S.H.; Mhareb, M.A.; Aziz, A.A.; Abu Noqta, O. A Novel Approach for Enhanced Osteosarcoma Photodynamic Therapy Using Encapsulated Methylene Blue in Silica Nanoparticles. *J. Compos. Sci.* **2023**, *7*, 137. <https://doi.org/10.3390/jcs7040137>

Academic Editors: Salvatore Brischetto and Francesco Tornabene

Received: 7 February 2023

Revised: 16 March 2023

Accepted: 29 March 2023

Published: 4 April 2023



Copyright: © 2023 by the authors. Licensee MDPI, Basel, Switzerland. This article is an open access article distributed under the terms and conditions of the Creative Commons Attribution (CC BY) license (<https://creativecommons.org/licenses/by/4.0/>).

Abstract: Photodynamic therapy (PDT) is a cutting-edge cancer treatment that utilizes both light and photosensitizers (PSs) to attack cancer cells. Methylene blue (MB) has emerged as a highly promising photosensitizer (PS) in PDT therapy due to its exceptional ability to produce singlet oxygen, which is attributed to its high quantum yield. However, the main challenge in utilizing MB in photodynamic therapy is its effective delivery to the target tissue. This challenge can be addressed by utilizing silica nanoparticles (SiNPs) as a drug delivery agent. Silica nanoparticles encapsulate MB and prevent its leakage, offering a novel approach to improving PDT therapy by reducing the toxicity of MB and increasing its bioavailability at the target cell. In this study, an extensive analysis of the size and shape evolution of the synthesized silica nanoparticles loaded with MB was conducted using TEM. Various encapsulated and bare MB concentrations were tested for cytotoxicity against osteosarcoma cells. Moreover, the optimal concentration and exposure time under light (with an intensity of approximately 8.9 mW/cm² in the visible range) were determined to achieve maximum cell elimination. The results revealed that encapsulated MB in SiNPs exhibited a higher efficacy compared to naked MB, with a 50% increase in concentration effectiveness and a 90% increase in exposure time efficacy. This confirms that encapsulated MB in SiNPs is more effective in killing osteosarcoma cells than bare MB, thereby enhancing photodynamic therapy through increased bioavailability of MB in target cells. The enhanced bioavailability of MB in target cells as a result of its encapsulation in SiNPs makes it a highly promising drug delivery candidate for significantly enhancing the efficacy of photodynamic therapy against osteosarcomas.

Keywords: photodynamic therapy; methylene blue; silica nanoparticles; encapsulation; osteosarcoma cells

1. Introduction

Over the past few years, extensive research has been conducted to improve the efficacy of photodynamic therapy (PDT) in treating cancer [1,2]. PDT therapy relies on two key components, a light source, and a photosensitizer (PS). By combining the two components together, PDT has the potential to be an effective cancer treatment with minimal side effects. By exposing the PS to light, the PS is activated and transfers its energy to oxygen

molecules, resulting in high production of reactive oxygen species (ROS) and, thus, cancer cell death [3]. ROS are highly reactive molecules that can damage cancer cells, leading to their death. This damage is localized to the cells that are exposed to light, meaning that the surrounding healthy cells are not affected. This results in minimal side effects compared to other cancer treatments. The challenge of delivering a sufficient amount of PS to the target tissue results in low ROS production efficiency. This difficulty is due to the reticuloendothelial system, which intercepts some of the PS molecules as part of the body's defense mechanism [4]. To tackle this challenge, researchers have been increasing their efforts to utilize silica nanoparticles, which are easily delivered and biocompatible to target cells [5–7]. Silica nanoparticles are small enough to penetrate cell membranes, and they can be engineered to carry drugs, genes, or other molecules directly to targeted cells. This allows for more precise and efficient delivery of the desired agents. The encapsulation properties of silica nanoparticles protect the PS during delivery and prevent it from interacting with the body's macrophages [8,9]. Silica nanoparticles have desirable characteristics that make them an ideal material for a drug delivery system (DDS). These include easy synthesis with low polydispersity at low temperatures, low toxicity, high biocompatibility, a tendency for biomolecular compounds to adhere to their outer surface, and the ability to encapsulate PS in their inner surface [10–12].

Methylene blue (MB) has emerged recently as a highly effective photosensitizer for photodynamic therapy due to its high quantum yield of reactive oxygen species generation and strong photocytotoxicity to tumor cells [13]. It is a second-generation phenothiazine dye with a therapeutic window between 600 and 900 nm, making it a promising candidate for PDT [14,15]. MB is also an inexpensive and widely used NIR fluorescent dye for bioanalysis [16]. However, naked MB in PDT has low efficiency, making its integration into nanoparticle-based systems an attractive option [14,15]. Encapsulated MB has been shown to improve PDT efficacy by providing better protection and delivery of the PS to the target tissue [17]. Nanoparticles loaded with MB can be further modified to enhance their targeting capabilities. Furthermore, the combination of silica nanoparticles and MB can reduce the side effects of PDT, such as toxicity and photobleaching. These nanosystems may also be utilized to deliver other agents in combination with MB in order to create synergistic effects. The reason for this is that they are capable of selectively targeting tumor cells, increasing the bioavailability of the photosensitizer, and increasing the rate at which the photosensitizer accumulates within the tumor. The silica nanoparticles also act as a protective layer around the photosensitizer, preventing it from being degraded before it can reach its target. Consequently, better control over the delivery of the photosensitizer can be achieved, thereby increasing the effectiveness of PDT.

Osteosarcoma is one of the most common bone tumors that threaten the lives of humans worldwide [18]. This type of cancer has a high metastatic potential and is most commonly found in adolescents and young adults. A child or young adult is most likely to develop this type of bone cancer as it is the most common type in this age group. A variety of treatment options are available, depending on the stage and location of the tumor. The disease usually begins in the bones, yet can spread to other areas of the body. Chemotherapy, surgery, and radiation therapy are some of the options for treatment. However, despite advancements in therapy [19,20], the long-term effectiveness of these treatments is limited by drug resistance and the likelihood of cancer recurrence [21,22]. Therefore, alternative treatments are actively being explored, such as immunotherapy, gene therapy, and targeted therapy. Additionally, researchers are focusing on developing new drugs and strategies to improve efficacy and reduce the side effects of existing therapies [23]. As a result, more effective treatments are required to eradicate osteosarcoma cells. In order to improve the long-term outcome of patients with osteosarcoma, novel therapies targeting more effective treatments are urgently needed. Therefore, increasing research efforts to improve existing therapies and develop novel treatments for osteosarcoma are essential for ensuring the best outcomes for patients.

In this study, the utilization of silica nanoparticles loaded with methylene blue (MB-SiNPs) was investigated to assess the potential benefits of encapsulating MB for photodynamic therapy of osteosarcoma. To the best of our knowledge, no previous research has been conducted on the effects of MB encapsulated by SiNPs on osteosarcoma. As part of this research, we evaluated the cytotoxicity of MB-SiNPs, determined the optimal concentration and exposure duration of MB-SiNPs, and compared the efficacy of encapsulated MB with bare MB in treating osteosarcoma cells at different concentrations and exposure durations. By preventing leakage of the photosensitizer, this innovative approach has the potential to reduce MB toxicity and increase its bioavailability to the target cells. The results of the study indicated that MB-SiNPs were more effective at treating osteosarcoma cells than bare MB, indicating that the encapsulation strategy was effective. Our research suggests that MB-SiNPs could be a promising strategy for targeted photodynamic therapy.

2. Materials and Method

The encapsulation of methylene blue by silica nanoparticles was performed using the reverse micellar method [24–26]. To start the process, 200 mL of distilled water, 0.1 mL of ammonia, and 5.5 g of Tween 80 were mixed and stirred for about 15 min. After verifying that the pH value of the solution was 9.0 at room temperature, 1-butanol was added and stirred for 5 min [27]. Then, the solution was transferred to a protected reactor covered with aluminum foil and 15 mL of MB was added and mixed at 320 rpm and 27 °C for 1 hour. In total, 2 mL of triethoxyvinylsilane (TEVS) was added and stirred under the same conditions for 20 h. The solution was dialyzed using a dialysis membrane for a few days to clear the nanoparticles, depending on the concentration of the photosensitizer [25].

The base concentration of MB used in the experiments was 15 mg/L (3.9 µM), which was then diluted 5 times. In total, 5 concentrations of MB (2.50, 1.25, 0.63, 0.31, 0.16, and 0 µM as the final concentration after filtration) were encapsulated with SiNPs [28]. Osteosarcoma cells (U-2 OS from ATCC) were removed from the minus 80 °C refrigerator, defrosted, and transferred from the cryogenic vial to a 15 mL plastic tube. The sample was mixed carefully with 6 mL of McCoy's medium, and the suspension solution was centrifuged at 2000 RPM for 15 min. The precipitated solution at the bottom of the centrifuge tube was the concentrated and cleaned cells. The osteosarcoma cells were cultured in the incubator for 6 hours at 37 °C in McCoy's medium containing 1% antibiotic (penicillin) and 10% fetal bovine serum (FBS) in a 5% CO₂ environment. The cells were then allowed to grow overnight. Phosphate-buffered saline (PBS) was used to wash the cells 3 times, then they were resuspended in 5 mL of fresh McCoy's medium containing MB-encapsulated SiNPs, at all MB concentrations [27]. All the samples were exposed to a light source (intensity approximately 8.9 mW/cm² from an arc lamp, with a 40 cm distance between the sample and the light source) for 60 min. After removing the medium, the cells were washed twice with PBS solution. A total of 3 mL of fresh McCoy's medium was added before placing the cells back in the incubator overnight. A manual method was used to count and determine cytotoxicity and the optimal concentration of MB-SiNPs. The process was repeated three times [28].

The morphological studies of the silica nanoparticles were conducted using transmission electron microscopy (TEM) and a Malvern Nano-ZS90 particle size analyzer. The hydrodynamic size measurements of the MB-SiNPs were performed and data were recorded at 0, 2, 4, and 6 days. An inverted light microscope and hemocytometer were used for cell counting. The cells were suspended in 4 mL of fresh medium, and 10 µL of the cells were mixed with 10 µL of trypan blue for 15 min. Then, 8 µL was inserted between the hemocytometer and its coverslip via a micropipette. The hemocytometer was fixed on the stage of the light microscope, and the cells were counted in 4 squares, each containing 16 small squares. The average sum of all counted cells (bright cells) was recorded and multiplied by 10⁴/4 to calculate the number of cells in 1 mL of the suspension sample. Cell viability was determined based on the ratio of living to dead cells in the total cell sample. Two samples of cells were used to measure cell viability. For the first sample, we used a

sample without any treatment with a photosensitizer or light source in order to determine the total number of untreated cells.

In the second sample, photodynamic therapy was applied to the sample. The ratio of the number of living cells in the treated sample to the number of living cells in the untreated sample, expressed as a percentage, is referred to as cell viability [27]. The cytotoxicity of the encapsulated MB-SiNPs on the osteosarcoma cells was measured by calculating the ratio of the number of untreated cells (as a control sample) to the number of treated cells (that were mixed with the encapsulated MB without a light source after incubating for 7 h in the incubator at 37 °C and 5% CO₂ environment). The half-maximal inhibitory concentration (IC₅₀) was determined.

The percentage of dead cells was measured by analyzing the cells treated with MB-SiNPs at various concentrations (2.50, 1.25, 0.63, 0.31, 0.16, and 0 μM), using a hemocytometer, to find the optimal concentration. The optimum exposure time was determined by exposing the optimal concentration to the light source for different durations (0, 15, 30, 45, 60, 75, 90, 105, and 120 min). Naked MB was also tested for 60 min, and the optimal concentration was exposed to the light for different exposure times (0, 15, 30, 45, 60, 75, 90, 105, 120, 135, and 150 min). The results of all MB-SiNPs were compared to the results of naked MB by measuring the concentration and exposure time efficacy using an efficacy equation [29]:

$$CE = [(C_{\text{encapsulated}} - C_{\text{naked}}) / C_{\text{encapsulated}}] \times 100\% \quad (1)$$

where CE represents concentration efficacy, $C_{\text{encapsulated}}$ represents the concentration of encapsulated MB, and C_{naked} represents the concentration of naked MB. Additionally, we used the same method to measure the effectiveness of the exposure time. To determine the impact of exposure time, we also observed the change in the concentration of encapsulated MB ($C_{\text{encapsulated}}$) and naked MB (C_{naked}) with respect to concentration efficacy (CE).

3. Results and Discussion

3.1. Characterization of the MB-SiNPs

The UV-vis spectrophotometer was used to analyze the spectrum of bare MB, as illustrated in Figure 1. The spectrum revealed that the maximum absorbance peak of MB was at a wavelength of 664 nm. To determine the power intensity of the radiation source during the photodynamic therapy experiment, the intensity was measured at a wavelength of 664 nm, which was approximately 8.9 mW/cm² from the arc lamp.

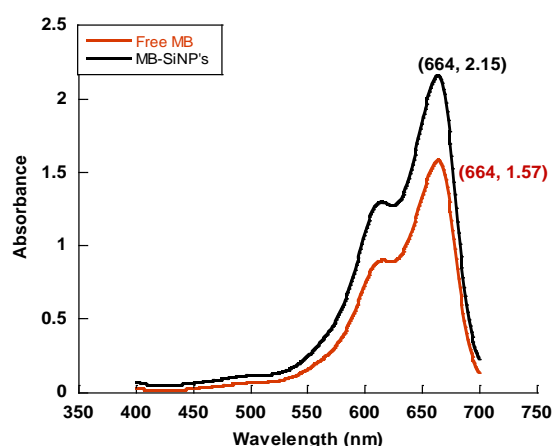


Figure 1. UV-vis spectrophotometer spectrum of naked MB and MB-SiNPs.

The morphological structures and particle sizes of the encapsulated MB by SiNPs were confirmed using TEM micrographs, as shown in Figure 2. The samples were found to be well-dispersed and spherical in shape, with an average diameter of approximately 26 nm. These results demonstrate that the MB molecules have been successfully encapsulated in

SiNPs. Furthermore, due to the small particle size of the SiNPs, the MB molecules will be more easily transported throughout the target cell. This ensures that the MB molecules will reach their desired target and be more effective in their therapeutic effects. In addition, the SiNPs provide a protective barrier for the MB molecules, shielding them from degradation and increasing their bioavailability. As such, encapsulating MB molecules in SiNPs provides an effective and reliable delivery system for MB molecules, leading to increased efficacy and decreased degradation.

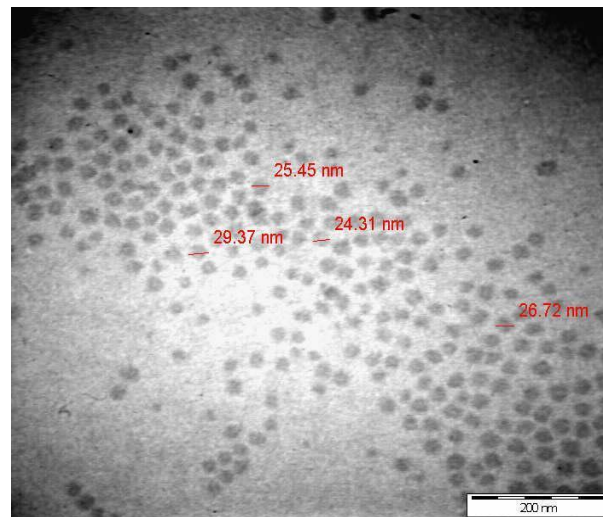


Figure 2. TEM visualization and analysis of methylene blue (MB) encapsulated within silica nanoparticles (SiNPs).

The hydrodynamic size of the NPs was measured using a zeta sizer machine multiple times within the first 6 days after synthesis to evaluate their stability. Figure 3 displays the average size of the SiNPs as approximately 28 nm. The results of the measurement indicate that the NPs remained stable, as the suspended solution showed no precipitate and no significant change in size. This highlights the high stability of the MB-SiNPs over the treatment time [30]. This result demonstrates the robustness of MB-SiNPs, providing assurance of their stability throughout treatment.

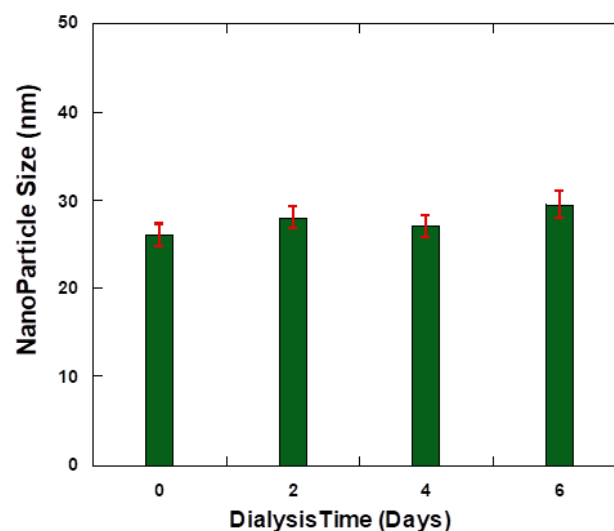


Figure 3. Particle size analysis of the SiNPs at several times during the first 6 days.

3.2. Cytotoxicity of Naked and Encapsulated MB on Osteosarcoma Cells

To determine the cytotoxicity of both bare and encapsulated MB on osteosarcoma cells, various concentrations of MB were incubated with the cells prior to conducting *in vitro* PDT studies. A total of 5 different concentrations of naked and encapsulated MB (0.16, 0.32, 0.64, 1.25, and 2.5 μM) were evaluated for their cytotoxicity on osteosarcoma cells. Figure 4 displays the results of the cytotoxicity test, showing the half-maximal inhibitory concentration (IC_{50}) for encapsulated MB was 0.81 μM and 2.45 μM for naked MB. Remarkably, the IC_{50} for encapsulated MB was lower than that of naked MB, indicating that the encapsulation protocol was successful in improving the cytotoxic properties of MB.

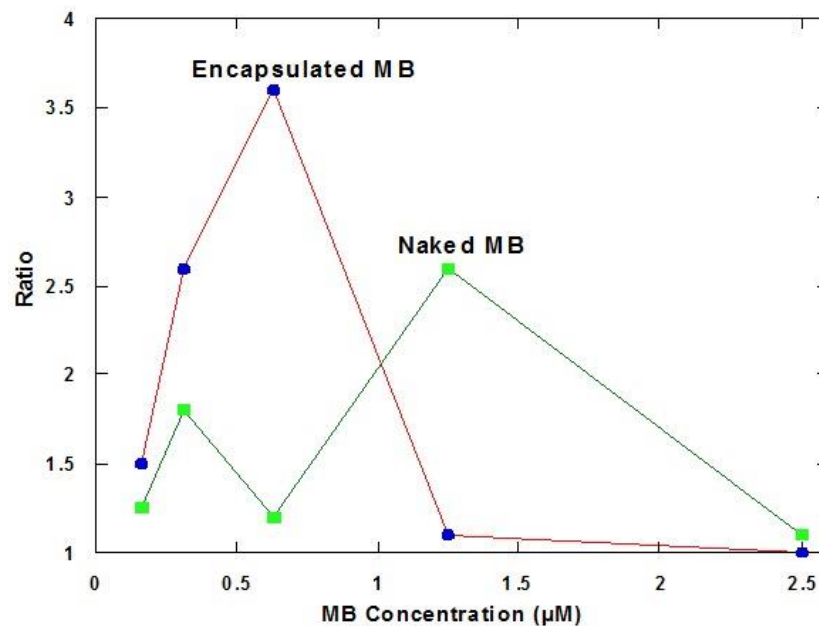


Figure 4. Cytotoxicity of bare and encapsulated MB on osteosarcoma cells at different concentrations.

The results indicated that naked MB had lower cytotoxicity compared to encapsulated MB. The higher cytotoxicity of encapsulated MB can be attributed to the outer surface of the silica nanoparticles. The silica nanoparticles form a protective shell around the MB molecules, preventing them from easily diffusing into the cells. This makes it difficult for the cells to recognize and process the MB molecules, which results in higher cytotoxicity. The toxicity of SiNPs to cells is dependent on their physicochemical properties and the type of cell [31]. Additionally, chemicals such as 1-Biotanol and Tween 80 that attached to the outer surface of SiNPs enhanced their cytotoxicity. Based on the results shown in Figure 4, concentrations below 0.81 μM for encapsulated MB and 2.45 μM for naked MB can be used effectively in PDT.

3.3. The Optimal Concentration of Encapsulated and Naked MB

The effects of MB-SiNPs at different concentrations (2.50, 1.25, 0.63, 0.31, 0.16, and 0 μM) on osteosarcoma cells were analyzed using a hemocytometer to determine the percentage of dead cells. Figure 5 displays the percentage of osteosarcoma cell death resulting from the incubation of different concentrations of naked and encapsulated MB with osteosarcoma cells, both in the absence and presence of light exposure. The results indicated that the cell death percentage increased with increasing concentrations of MB-SiNPs and that cell death was more pronounced when MB-SiNPs were exposed to light. The samples exposed to light were subjected to continuous irradiation for 120 min.

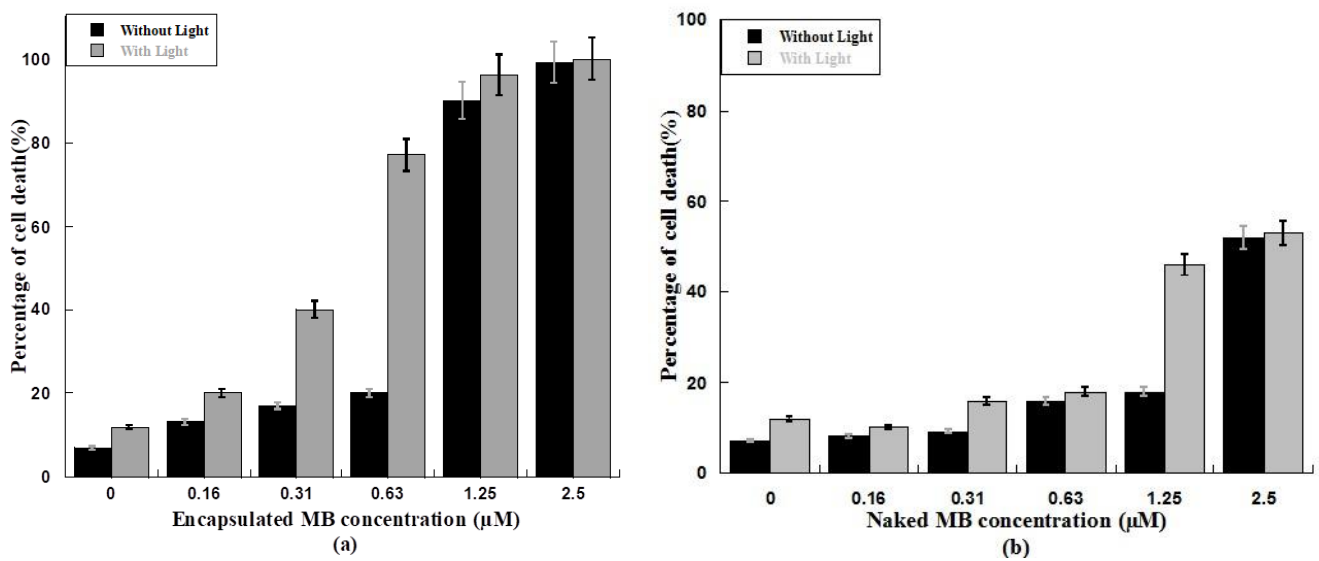


Figure 5. Comparison of cell death percentage with and without irradiation for (a) MB encapsulated within SiNPs and (b) naked MB.

For encapsulated MB-SiNPs, the results indicated that in the dark, the cytotoxicity of these MB-SiNPs was greater than 50% for concentrations of 1.25 and 2.50 μM. However, under light exposure conditions, the MB-SiNPs, with concentrations of 0.63, 1.25, and 2.50 μM, destroyed more than 50% of the cells (as seen in Figure 5a). According to these results, MB-SiNPs can be utilized as an effective antiosteosarcoma agent when combined with light to target tumor cells.

The comparison of dead cell percentage under light irradiation to that under dark conditions confirmed that the optimal concentration for MB-SiNPs with the maximum ratio was 0.63 μM, as shown in Figure 6. Regarding naked MB, the results showed that in the dark, the cytotoxicity of naked MB was greater than 50% for the concentration of 2.50 μM. However, under light exposure conditions, naked MB with concentrations of 1.25 and 2.50 μM destroyed more than 50% of the cells (as seen in Figure 5b).

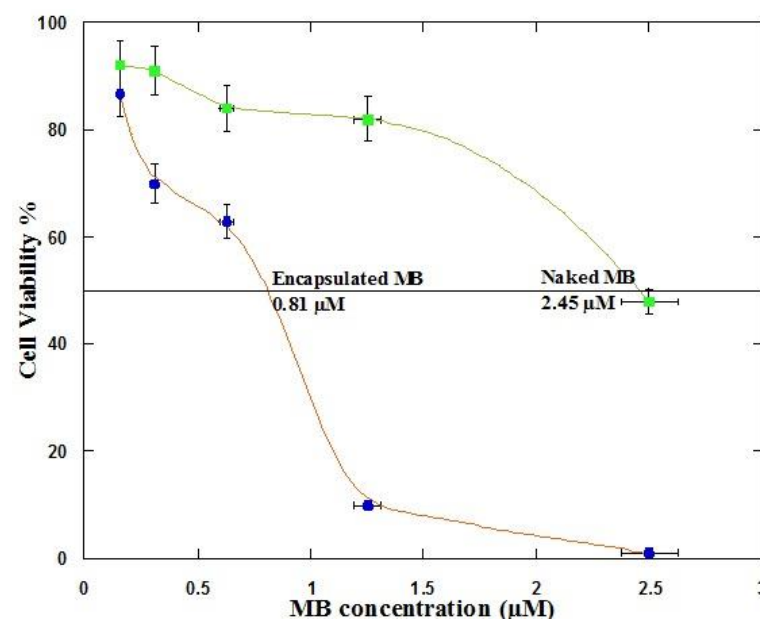


Figure 6. The ratio of percentage cell death under light irradiation to that without light irradiation for encapsulated and naked MB.

According to Figure 6, based on a comparison of dead cell percentages under light irradiation and dark conditions, 1.25 M is the optimal concentration for naked MB with the maximum ratio. The results suggest that the concentration of encapsulated MB needed to achieve the same destruction efficiency for osteosarcoma cells was about half that of naked MB. Hence, the concentration efficacy was calculated to be 50% using the efficacy equation. However, in the presence of light, the percentage of dying cells increased as both naked and encapsulated MB concentrations were elevated over time. As a result, the production of singlet oxygen and reactive oxygen species was enhanced by exposure to light [32–34]. Similarly, cytotoxicity produced without light increased with an increase in MB concentrations. These findings indicate that light and MB concentrations can both contribute to the excessive production of reactive oxygen species, leading to enhanced cytotoxicity.

3.4. The Optimal Exposure Time for Encapsulated and Naked MB

The time dependence of the treatment for encapsulated and naked MB was measured using the optimal concentrations obtained in the previous section. Experiments were conducted using 0.63 μM of encapsulated MB and 1.25 μM of naked MB on osteosarcoma cells.

Encapsulated MB was exposed to light at various exposure times (0, 15, 30, 45, 60, 75, 90, 105, and 120 min), as illustrated in Figure 7a. Using the results shown in Figure 7c, it can be concluded that approximately 41 min was the optimal time for 50% of the osteosarcoma cells to be destroyed. However, exposing naked MB to the same 10 different durations revealed that it took 78 min to kill 50% of the cells, as depicted in Figure 7c. This indicates that encapsulated MB was more effective at destroying the target cells, requiring less exposure time compared to naked MB. The exposure time efficacy was calculated using the efficacy equation as 90%. This provides a clear illustration of the effectiveness of encapsulated MB, as it has demonstrated 90% efficacy even when exposing it for shorter periods of time.

As a treatment, the photodynamic effect required a lower concentration of encapsulated MB than naked MB to achieve the same level of toxicity on osteosarcoma cells. On the other hand, the photodynamic effect of naked MB required a longer exposure time to kill half of the target cells using the optimal MB concentration compared to encapsulated MB. Irradiation with light resulted in effective damage to the cancer cells due to the increased absorption of light and singlet oxygen production in ROS by encapsulated MB molecules, which are collected together by the encapsulation in SiNPs, compared to naked MB, which is dispersed in solution. As a result, its interaction with light and its effects were weaker and dispersed [24,35].

As a treatment, to achieve the same level of toxicity on osteosarcoma cells, the photodynamic effect of MB encapsulated required a lower concentration of MB than bare MB. On the other hand, the photodynamic effect of bare MB required a longer exposure time to kill half of the target cells using the optimal MB concentration compared to encapsulated MB. Irradiation with light resulted in effective damage to the cancer cells due to increased absorption of light and singlet oxygen production in ROS, as a result of encapsulated MB molecules being collected together by their encapsulation in SiNPs, compared to naked MB being dispersed in solution. In this case, MB molecules encapsulated in a small area of the cell are unable to move around freely. Therefore, the same amount of light can cause more photochemical reactions than what occurs with free MB molecules, which are dispersed in solution. This, ultimately, results in more effective damage to cancer cells. As a result, its interaction with light and its effects were stronger and more concentrated compared to bare MB [24,34]. This makes photodynamic therapy with MB-SiNPs more efficient and effective, leading to improved PDT treatment outcomes.

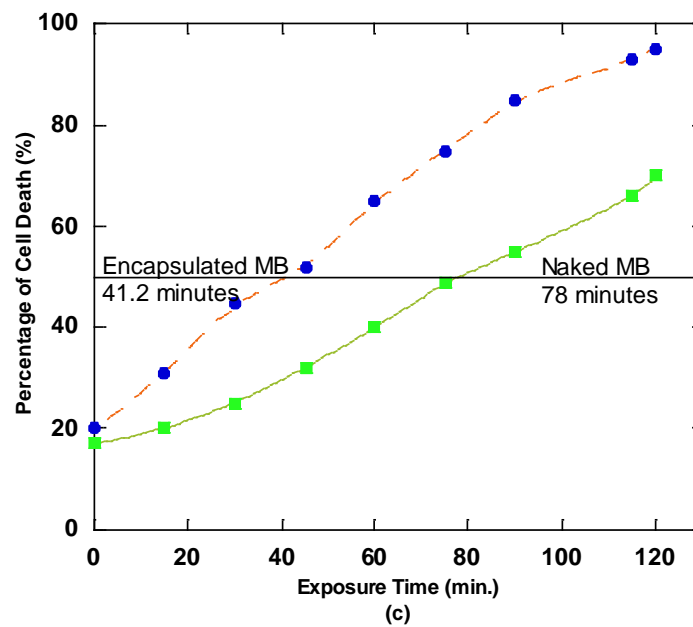
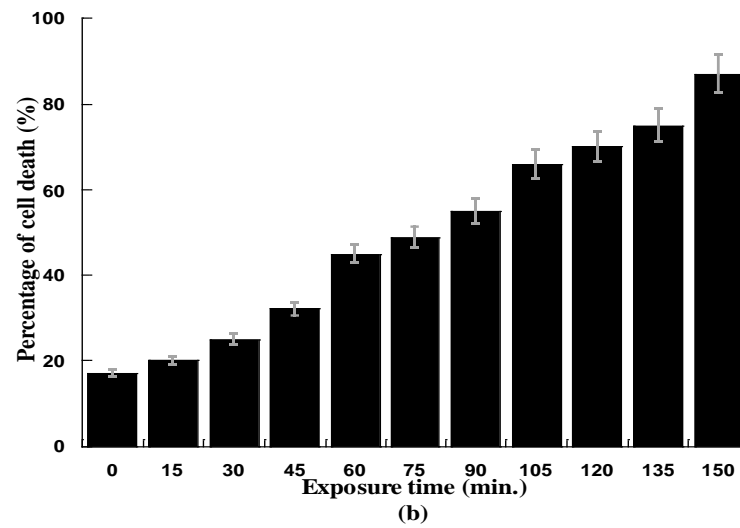
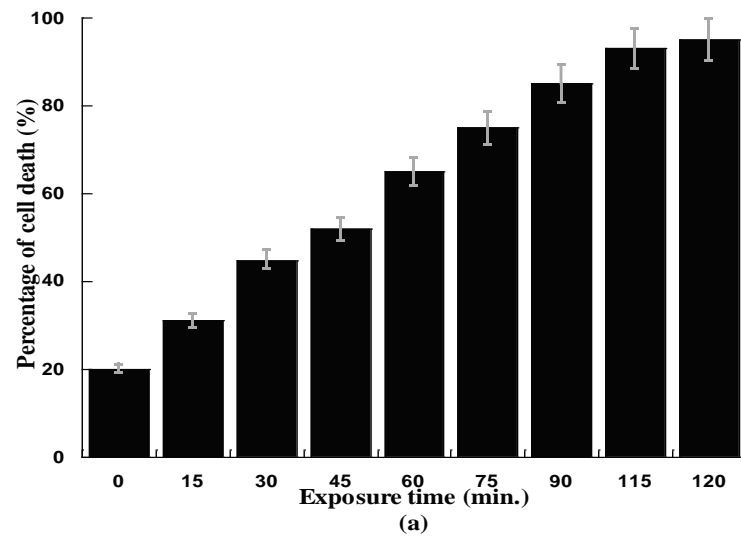


Figure 7. The time dependence of the treatment by using the optimal concentration for (a) encapsulated MB and (b) naked MB. (c) The optimum exposure time for the treatment.

4. Conclusions

In conclusion, this study has significantly contributed to advancing the field of photodynamic therapy by demonstrating that MB encapsulated in SiNPs is more effective against osteosarcoma. The research findings indicate that encapsulation of MB allows for better light penetration, leading to an increase in the production of reactive oxygen species (ROS). The results indicated that encapsulated MB was more effective, with an optimal concentration of 0.63 M and exposure time of 41 min, in comparison to naked MB, which required a higher concentration of 1.25 M and a longer exposure time of 78 min. The ROS generated by encapsulated MB led to the death of cancer cells, while leaving healthy cells unharmed. This indicates that encapsulated MB could have potential as a targeted treatment for cancer. The findings of this study are expected to have significant implications for the treatment of cancer in the future, particularly in terms of photodynamic therapy. The achievement of this research opens up new avenues for exploring the potential of photodynamic therapy in a variety of cancer treatments by improving the delivery and efficacy of MB through nanoparticle encapsulation.

Author Contributions: Funding acquisition, K.A.J. and M.-A.H.A.-A.; Investigation, K.A.J., M.-A.H.A.-A., G.N.M. and T.A.; Supervision, K.A.J. and M.-A.H.A.-A.; Project administration, K.A.J. and M.-A.H.A.-A.; Writing—review & editing, K.A.J., M.-A.H.A.-A., G.N.M., O.A.N., T.A., A.A., S.H.Z., M.A.M., A.A.A. and O.A.N.; Writing—original draft, G.N.M. and T.A.; Methodology, G.N.M., K.A.J. and T.A.; Formal analysis, G.N.M., O.A.N., T.A., A.A., S.H.Z., M.A.M. and A.A.A.; Conceptualization, G.N.M., K.A.J. and T.A.; Data curation, G.N.M.; Visualization, G.N.M., O.A.N. and T.A.; Validation, K.A.J., M.-A.H.A.-A., G.N.M., O.A.N., T.A., A.A., S.H.Z., M.A.M., A.A.A. and O.A.N. All authors have read and agreed to the published version of the manuscript.

Funding: This research was funded by Deanship of Research at Jordan University of Science and Technology grant number 202/2022 And The APC was funded by American University of the Middle East in Kuwait.

Acknowledgments: The authors would like to thank the Deanship of Research at Jordan University of Science and Technology for supporting and funding this research project (Grant # 202/2022).

Conflicts of Interest: The authors declare no conflict of interest.

References

- Schuitmaker, J.J.; Baas, P.; van Leengoed, H.L.; van der Meulen, F.W.; Star, W.M.; van Zandwijk, N. Photodynamic Therapy: A Promising New Modality for the Treatment of Cancer. *J. Photochem. Photobiol. B* **1996**, *34*, 3–12. [[CrossRef](#)] [[PubMed](#)]
- Zhao, X.; Liu, J.; Fan, J.; Chao, H.; Peng, X. Recent Progress in Photosensitizers for Overcoming the Challenges of Photodynamic Therapy: From Molecular Design to Application. *Chem. Soc. Rev.* **2021**, *50*, 4185–4219. [[CrossRef](#)] [[PubMed](#)]
- Al Akhras, M.A.H. Introducing the Effect of Chinese Chlorella as a Photosensitizing Drug at Different Temperatures. *J. Mol. Pharm. Org. Process Res.* **2013**, *1*, e109. [[CrossRef](#)]
- Tang, W.; Xu, H.; Park, E.J.; Philbert, M.A.; Kopelman, R. Encapsulation of Methylene Blue in Polyacrylamide Nanoparticle Platforms Protects Its Photodynamic Effectiveness. *Biochem. Biophys. Res. Commun.* **2008**, *369*, 579–583. [[CrossRef](#)] [[PubMed](#)]
- Wilczewska, A.Z.; Niemirowicz, K.; Markiewicz, K.H.; Car, H. Nanoparticles as Drug Delivery Systems. *Pharm. Rep.* **2012**, *64*, 1020–1037. [[CrossRef](#)]
- Xiong, R.; Hua, D.; Van Hoeck, J.; Berdecka, D.; Léger, L.; De Munter, S.; Fraire, J.C.; Raes, L.; Harizaj, A.; Sauvage, F.; et al. Photothermal Nanofibres Enable Safe Engineering of Therapeutic Cells. *Nat. Nanotechnol.* **2021**, *16*, 1281–1291. [[CrossRef](#)]
- Abuelsamen, A.; Mahmud, S.; Mohd Kaus, N.H.; Farhat, O.F.; Mohammad, S.M.; Al-Suede, F.S.R.; Abdul Majid, A.M.S. Novel Pluronic F-127-Coated ZnO Nanoparticles: Synthesis, Characterization, and Their in-Vitro Cytotoxicity Evaluation. *Polym. Adv. Technol.* **2021**, *32*, 2541–2551. [[CrossRef](#)]
- Bharali, D.J.; Klejbor, I.; Stachowiak, E.K.; Dutta, P.; Roy, I.; Kaur, N.; Bergey, E.J.; Prasad, P.N.; Stachowiak, M.K. Organically Modified Silica Nanoparticles: A Nonviral Vector for in Vivo Gene Delivery and Expression in the Brain. *Proc. Natl. Acad. Sci. USA* **2005**, *102*, 11539–11544. [[CrossRef](#)]
- Xiong, R.; Xu, R.X.; Huang, C.; Smedt, S.D.; Braeckmans, K. Stimuli-Responsive Nanobubbles for Biomedical Applications. *Chem. Soc. Rev.* **2021**, *50*, 5746–5776. [[CrossRef](#)]
- Kneuer, C.; Sameti, M.; Haltner, E.G.; Schiestel, T.; Schirra, H.; Schmidt, H.; Lehr, C.M. Silica Nanoparticles Modified with Aminosilanes as Carriers for Plasmid DNA. *Int. J. Pharm.* **2000**, *196*, 257–261. [[CrossRef](#)]
- Santra, S.; Yang, H.; Dutta, D.; Stanley, J.T.; Holloway, P.H.; Tan, W.; Moudgil, B.M.; Mericle, R.A. TAT Conjugated, FITC Doped Silica Nanoparticles for Bioimaging Applications. *Chem. Commun.* **2004**, *24*, 2810–2811. [[CrossRef](#)]

12. Ma, Q.; Sun, X.; Wang, W.; Yang, D.; Yang, C.; Shen, Q.; Shao, J. Diketopyrrolopyrrole-derived Organic Small Molecular Dyes for Tumor Phototheranostics. *Chin. Chem. Lett.* **2022**, *33*, 1681–1692. [CrossRef]
13. A Compilation of Singlet Oxygen Yields from Biologically Relevant Molecules-PubMed. Available online: <https://pubmed.ncbi.nlm.nih.gov/10546544/> (accessed on 1 April 2023).
14. Methylene Blue in Place of Acridine Orange as a Photosensitizer in Photodynamic Therapy of Osteosarcoma-PubMed. Available online: <https://pubmed.ncbi.nlm.nih.gov/18610739/> (accessed on 1 April 2023).
15. Photodynamic Action of Methylene Blue in Osteosarcoma Cells in Vitro-PubMed. Available online: <https://pubmed.ncbi.nlm.nih.gov/24629696/> (accessed on 1 April 2023).
16. Targeting Autophagy Potentiates Chemotherapy-Induced Apoptosis and Proliferation Inhibition in Hepatocarcinoma Cells-PubMed. Available online: <https://pubmed.ncbi.nlm.nih.gov/22406827/> (accessed on 1 April 2023).
17. He, X.; Wu, X.; Wang, K.; Shi, B.; Hai, L. Methylene Blue-Encapsulated Phosphonate-Terminated Silica Nanoparticles for Simultaneous in Vivo Imaging and Photodynamic Therapy. *Biomaterials* **2009**, *30*, 5601–5609. [CrossRef]
18. Tian, Z.; Quan, X.; Leung, A.W.; Xiang, J.; Xu, C. Hematoporphyrin Monomethyl Ether Enhances the Killing of Ultrasound on Osteosarcoma Cells Involving Intracellular Reactive Oxygen Species and Calcium Ion Elevation. *Integr. Cancer* **2010**, *9*, 365–369. [CrossRef]
19. Gorlick, R.; Anderson, P.; Andrulis, I.; Arndt, C.; Beardsley, G.P.; Bernstein, M.; Bridge, J.; Cheung, N.-K.; Dome, J.S.; Ebb, D.; et al. Biology of Childhood Osteogenic Sarcoma and Potential Targets for Therapeutic Development: Meeting Summary. *Clin. Cancer Res.* **2003**, *9*, 5442–5453.
20. Bacci, G.; Longhi, A.; Fagioli, F.; Briccoli, A.; Versari, M.; Picci, P. Adjuvant and Neoadjuvant Chemotherapy for Osteosarcoma of the Extremities: 27 Year Experience at Rizzoli Institute, Italy. *Eur. J. Cancer* **2005**, *41*, 2836–2845. [CrossRef]
21. Bielack, S.S.; Kempf-Bielack, B.; Delling, G.; Exner, G.U.; Flege, S.; Helmke, K.; Kotz, R.; Salzer-Kuntschik, M.; Werner, M.; Winkelmann, W.; et al. Prognostic Factors in High-Grade Osteosarcoma of the Extremities or Trunk: An Analysis of 1,702 Patients Treated on Neoadjuvant Cooperative Osteosarcoma Study Group Protocols. *J. Clin. Oncol.* **2002**, *20*, 776–790. [CrossRef]
22. Survival from High-Grade Localised Extremity Osteosarcoma: Combined Results and Prognostic Factors from Three European Osteosarcoma Intergroup Randomised Controlled Trials-PMC. Available online: <https://www.ncbi.nlm.nih.gov/pmc/articles/PMC3360547/> (accessed on 1 April 2023).
23. Zhao, X.; Wu, Q.; Gong, X.; Liu, J.; Ma, Y. Osteosarcoma: A Review of Current and Future Therapeutic Approaches. *BioMedical Eng. Online* **2021**, *20*, 24. [CrossRef]
24. Roy, I.; Ohulchanskyy, T.Y.; Pudavar, H.E.; Bergey, E.J.; Oseroff, A.R.; Morgan, J.; Dougherty, T.J.; Prasad, P.N. Ceramic-Based Nanoparticles Entrapping Water-Insoluble Photosensitizing Anticancer Drugs: A Novel Drug–Carrier System for Photodynamic Therapy. *J. Am. Chem. Soc.* **2003**, *125*, 7860–7865. [CrossRef]
25. Chatterjee, D.K.; Fong, L.S.; Zhang, Y. Nanoparticles in Photodynamic Therapy: An Emerging Paradigm. *Adv. Drug Deliv. Rev.* **2008**, *60*, 1627–1637. [CrossRef]
26. Makhadmeh, G.N.; Aziz, A.A.; Razak, K.A.; Al-Akhras, M.-A.H. Effect of Photon Radiations in Semi-Rigid Artificial Tissue Sensitized by Protoporphyrin IX Encapsulated with Silica Nanoparticles. *Conf. Ser. Mater. Sci. Eng.* **2018**, *305*, 012014. [CrossRef]
27. Makhadmeh, G.N.; Abuelsamen, A.; Al-Akhras, M.-A.H.; Aziz, A.A. Silica Nanoparticles Encapsulated Cichorium Pumulom as a Promising Photosensitizer for Osteosarcoma Photodynamic Therapy: In-Vitro Study. *Photodiagnosis Photodyn.* **2022**, *38*, 102801. [CrossRef] [PubMed]
28. Makhadmeh, G.N.; Abdul Aziz, A.; Abdul Razak, K.; Abu Noqta, O. Encapsulation Efficacy of Natural and Synthetic Photosensitizers by Silica Nanoparticles for Photodynamic Applications. *IET Nanobiotechnol.* **2015**, *9*, 381–385. [CrossRef] [PubMed]
29. Erickson, A.J.; Weiss, P.T.; Gulliver, J.S. *Stormwater Treatment: Assessment and Maintenance*; St. Anthony Falls Laboratory: Minneapolis, MN, USA, 2010.
30. Aditya, A.; Chattopadhyay, S.; Jha, D.; Gautam, H.K.; Maiti, S.; Ganguli, M. Zinc Oxide Nanoparticles Dispersed in Ionic Liquids Show High Antimicrobial Efficacy to Skin-Specific Bacteria. *ACS Appl. Mater. Interfaces* **2018**, *10*, 15401–15411. [CrossRef]
31. The Toxicity of Silica Nanoparticles to the Immune System | Nanomedicine. Available online: <https://www.futuremedicine.com/doi/10.2217/nnm-2018-0076> (accessed on 1 April 2023).
32. Makhadmeh, G.N.; Aziz, A.A.; Razak, K.A. Loading and Unloading Properties of Encapsulated Methylene Blue in Silica Nanoparticles for Photodynamic Applications. *Adv. Mater. Res.* **2014**, *1024*, 292–295. [CrossRef]
33. Alzoubi, F.Y.; Abu Noqta, O.; Al Zoubi, T.; Al-Khateeb, H.M.; Alqadi, M.K.; Abuelsamen, A.; Makhadmeh, G.N. A Novel One-Pot Synthesis of PVP-Coated Iron Oxide Nanoparticles as Biocompatible Contrast Agents for Enhanced T2-Weighted MRI. *J. Compos. Sci.* **2023**, *7*, 131. [CrossRef]
34. Benyoucef, M.; Usman, M.A.U.; Alzoubi, T.; Reithmaier, J.P. Pre-patterned Silicon Substrates for the Growth of III–V Nanostructures. *Phys. Status Solidi* **2012**, *209*, 2402–2410. [CrossRef]
35. Makhadmeh, G.N.; Abdul Aziz, A. Photodynamic Application of Protoporphyrin IX as a Photosensitizer Encapsulated by Silica Nanoparticles. *Artif. Cells Nanomed. Biotechnol.* **2018**, *46*, S1043–S1046. [CrossRef]

Disclaimer/Publisher’s Note: The statements, opinions and data contained in all publications are solely those of the individual author(s) and contributor(s) and not of MDPI and/or the editor(s). MDPI and/or the editor(s) disclaim responsibility for any injury to people or property resulting from any ideas, methods, instructions or products referred to in the content.